Biochemical and Biophysical Research Communications 418 (2012) 396–401

Contents lists available at SciVerse ScienceDirect

Biochemical and Biophysical Research Communications

journal homepage: www.elsevier.com/locate/ybbrc

The quorum sensing transcriptional regulator TraR has separate binding sites for DNA and the anti-activator

Zhida Zheng, Clay Fuqua, Lingling Chen *

Department of Molecular and Cellular Biochemistry, 212 S. Hawthorne Dr. Simon Hall 400A, Indiana University, Bloomington, IN 47405, USA

ARTICLE INFO

Article history:
Received 13 December 2011
Available online 17 January 2012

Keywords:
Quorum sensing antiactivation
TraR–TraM interaction
TraR–DNA interaction
ITC studies
EMSA studies

ABSTRACT

Quorum sensing represents a mechanism by which bacteria control their genetic behaviors *via* diffusible signals that reflect their population density. TraR, a quorum sensing transcriptional activator in the *Rhizobiaceae* family, is regulated negatively by the anti-activator TraM *via* formation of a TraR–TraM heterocomplex. Prior structural analysis suggests that TraM and DNA bind to TraR in distinct sites. Here we combined isothermal titration calorimetry (ITC) and electrophoretic mobility shift assays (EMSA) to investigate roles of TraR residues from *Rhizobium* sp. NGR234 in binding of both TraM and DNA. We found that K213A mutation of $TraR_{NGR}$ abolished DNA binding, however, did not alter TraM binding. Mutations of TraM-interfacing $TraR_{NGR}$ residues decreased the TraR–TraM interaction, but did not affect the DNA-binding activity of $TraR_{NGR}$. Thus, our biochemical studies support the independent binding sites on TraR for TraM and DNA. We also found that point mutations in $TraR_{NGR}$ appeared to decrease the TraR–TraM interaction more effectively than those in $TraM_{NGR}$, consistent with structural observations that individual $TraR_{NGR}$ residues contact with more $TraM_{NGR}$ residues than each $TraM_{NGR}$ residues with $TraR_{NGR}$ residues. Finally, we showed that TraM inhibition on DNA-binding of TraR was driven thermodynamically. We discussed subtle mechanistic differences in TraM anti-activation on TraR activity between homologous systems.

1. Introduction

Quorum sensing is a signal transduction mechanism by which bacteria communicate among themselves to coordinate population-dependent community behaviors [1–3]. Quorum sensing has been found to regulate a variety of biological processes including bioluminescence, biofilm formation, plasmid transfer, virulence gene expression, production of exoenzymes and antibiotics, and surface motility. The signal molecules used by many gram-negative members of the *Proteobacteria* are acyl-homoserine lactones (acyl-HSLs). Most acyl-HSLs are synthesized by LuxI-type enzymes in the cytoplasm [4–6], and diffuse across the cell membrane either passively [7] or with the assistance of general efflux systems [8]. Acyl-HSL concentrations are proportional to the population of their producing cells. When bacteria attain a certain population density, as monitored by an AHL concentration threshold, acyl-HSLs are recognized by LuxR-type receptors [4]. LuxR-type proteins are transcription factors that interact directly with promoter regions of the controlled genes; association with acyl-HSLs regulates their DNA binding activity (see [9] and references therein). The DNA sequences recognized by LuxR-type proteins, termed the *lux*-like boxes [10], are 18–20 bp imperfect palindromic sequences.

$TraR_{At}$ [11,12] of *Agrobacterium tumefaciens*, a member of the *Rhizobiaceae* family, represents the best biochemically and structurally characterized LuxR-type protein (see [9,13]). $TraR_{At}$ exists as a homodimer, and each monomer folds into two domains. The N-terminal domain (NTD) contains the binding site for its cognate ligand *N*-(3-oxo-octanoyl)-L-homoserine lactone (3-oxo-C8-HSL), and the C-terminal domain (CTD) interacts with DNA. The two domains are tethered *via* a structurally flexible linker of ~12 amino acid residues. The signal acyl-HSL is completely buried within a hydrophobic pocket of the NTD residues, suggesting its role as a folding scaffold for stabilizing the $TraR_{At}$ structure [14,15], consistent with its ability to maintain $TraR_{At}$ in a soluble stable state [16]. The $TraR_{At}$ CTD is comprised of a helix-turn-helix structure, the widespread DNA-binding motif, and the DNA-interacting helix, α12 (numbering according to [14]), binds to the major groove of the *tra*-box DNA [14,15]. In particular, side chains of R206 and R210, make specific contacts with the base components of the DNA sequence, conferring specific DNA recognition by $TraR_{At}$.

TraR activity may be antagonized by protein–protein interactions with antiactivators including TraM [17,18]. $TraM_{At}$ prevents $TraR_{At}$ from binding to DNA, and displaces $TraR_{At}$ from pre-formed TraR–DNA complexes; thereby inhibiting TraR activity [19–21]. $TraM_{At}$ interacts with $TraR_{At}$ CTD [19]; however crystal structure of the TraR–TraM complex from *Rhizobium* sp. NGR234, also a member of the *Rhizobiaceae* family, indicate that most of the TraM-interacting

* Corresponding author. Fax: +1 812 855 6082.
E-mail address: linchen@indiana.edu (L. Chen).

0006-291X/$ - see front matter © 2012 Elsevier Inc. All rights reserved.
doi:10.1016/j.bbrc.2012.01.035

residues are not located on the DNA recognition helix α12 [22]. In this study, we identified the DNA-binding residue in $TraR_{NGR}$, and found it is located away from the $TraR_{NGR}$–$TraM_{NGR}$ interface revealed from the structure of $TraR_{NGR}$–$TraM_{NGR}$. We further conducted biochemical analyses to confirm that the $TraR_{NGR}$ residue important for DNA binding is different from those for $TraM_{NGR}$ binding. In addition, we examined the contributions of both $TraR_{NGR}$ and $TraM_{NGR}$ residues to the TraR–TraM interaction. Finally, we analyzed the driving force for TraM to prevent TraR from binding to DNA.

2. Materials and methods

2.1. Protein expression and purification

The *traR* coding sequence of *Rhizobium* sp. strain NGR234 was ligated *via* *Nde*I/*Eco*RI sites into pRSETA (Invitrogen) in which the N-terminal His_6-tag was removed, and the *traM* coding sequence was ligated *via* *Nde*I/*Bam*HI sites into pET15b (Novagen). *Escherichia coli* Rosetta 2 and BL21(DE3) cells (Novagen) were transformed with the $traR_{NGR}$ and $traM_{NGR}$ plasmids, respectively. Point mutations were performed using QuickChange Kit (Stratagene). To overexpress $TraR_{NGR}$, cells were grown in LB to an optical density at 600 nm (OD_{600}) of 0.6 at 37 °C, and 3-oxo-C8-HSL and isopropyl-β-D-thiogalactopyranoside (IPTG) were added to final concentrations of 25 μM and 0.1 mM, respectively. Cells were allowed to grow for 12 h at 16 °C. To overexpress $TraM_{NGR}$, cells were grown in LB to an OD_{600} of 0.8 at 37 °C, and induced for 5 h with IPTG (to a final concentration of 0.4 mM).

To purify $TraR_{NGR}$, cells were lysed in Buffer A (50 mM imidazole, pH 8.0, 0.5 mM EDTA, 300 mM NaCl, 1 mM β-mercaptoethanol, and 5% glycerol), using a continuous flow microfluidizer (Microfluidics). The clear lysate was loaded onto a heparin column (Amersham Biosciences) and eluted with a gradient of 300–1000 mM NaCl. $TraR_{NGR}$-containing fractions were separated by a FastS column (Amersham Biosciences) in Buffer A with a gradient of 300–1000 mM NaCl, and were further purified by a Superdex200 column (Amersham Biosciences) in Buffer B (Buffer A except that NaCl was 1 M).

To purify $TraM_{NGR}$, cells were lysed in Buffer C (50 mM sodium phosphate, pH 8.0, 5 mM imidazole, and 300 mM NaCl), using the microfluidizer. The clear cell lysate was loaded on a Ni affinity column (Amersham Biosciences), and eluted with a gradient of imidazole (5–500 mM). $TraM_{NGR}$-containing sample was separated by a FastQ column (Amersham Biosciences) in Buffer D (50 mM sodium phosphate, pH 8.0, 0.5 mM EDTA, 1 mM β-mercaptoethanol, and 50 mM NaCl) with a gradient of 50–1000 mM NaCl, and was further purified by a Superdex75 column (Amersham Biosciences) in Buffer E (50 mM TriCl, pH 8.0, 20 mM NaCl, 0.5 mM EDTA, and 1 mM β-mercaptoethanol).

2.2. Isothermal titration calorimetry (ITC) experiments

To anneal the 20-bp double-stranded DNA (*tra* box II) for ITC studies, 200 μl of 1 μM 5′-CCTTGTAGGATCCTACAACT-3′, 200 μl 1 μM 5′-AGTTGTAGGATCCT ACCAAGG-3′, and 200 μl 1 M $MgCl_2$ were mixed in 400 μl annealing buffer (10 mM TrisCl, 50 mM NaCl, 1 mM EDTA, pH 8.0). The mixture was heated to 98 °C for 2 min, and was slowly cooled down to room temperature overnight. The product was dialyzed extensively using a dialysis cassette of 3 K MWCO (Pierce) to the ITC buffer (50 mM imidazole, pH 7.0, 0.5 mM EDTA, 300 mM NaCl, and 1 mM β-mercaptoethanol), and stored in −20 °C.

ITC experiments were carried out at 25 °C in a MicroCal VP-ITC titration calorimeter system (MicroCal). To study DNA binding of $TraR_{NGR}$ mutants, 30 injections of 10 μl of the 20-bp DNA (50 μM) were titrated to 1.4 ml of $TraR_{NGR}$ (8 μM) at 360-s intervals. To study $TraM_{NGR}$ binding of $TraR_{NGR}$ mutants, 30 injections of 10 μl of $TraR_{NGR}$ (40 μM) were titrated to 1.4 ml of $TraM_{NGR}$ (5 μM) at 240-s intervals. To study $TraR_{NGR}$ binding of $TraM_{NGR}$ mutants, 30 injections of 10 μl of $TraR_{NGR}$ (40 μM) were titrated to 1.4 ml of $TraM_{NGR}$ mutants (5 μM) at 240-s intervals. Data were processed using the Origin software (Origin Lab), and thermodynamic parameters of the binding process were derived by fitting the corrected binding isotherm to a single-site binding model.

2.3. Electrophoretic mobility shift assay (EMSA)

The infrared dye (IR)-labeled *traI* promoter (558-bp DNA) of *Rhizobium* sp. Strain NGR234 was generated using two primers: 5′-TGAATATATTCGAGTTCTGAGTTGC-3′ (Integrated DNA Technologies) and 5′-ATGGCTGCGGAGAAGTTGGG-3′ (IRD800 labeled; MWG Biotech). This fragment extends from −471 to +87 bp of the *traI* transcription start site. The PCR products were purified using PCR Purification Kit (Qiagen). Different amounts of $TraR_{NGR}$ were incubated with 100 nM IR-labeled full-length promoter DNA in reaction buffer (4 mM TrisCl, pH 8.0, 12 mM NaHepes 1 mM EDTA, 1 mM DTT, 60 mM potassium glutamate, 0.1 mg/ml BSA, and 12% glycerol) at 4 °C overnight. The reactions were electrophoretically separated using a 5.2% non-denaturing polyacrylamide gel in 25 mM glycine, pH 10.5. The gel band intensities were digitized using the Odyssey infrared image system (Li-COR).

3. Results

3.1. TraR specifically interacts with the tra box II sequence

The Dtr (DNA transfer and replication) and Mpf (Mating pair formation) genes on plasmid pNGR234a of *Rhizobium* sp. NGR234 are essential for conjugal transfer, and are under the control of quorum sensing transcription factor $TraR_{NGR}$ [23]. Three DNA regions are potential for $TraR_{NGR}$ binding: *tra* box I of the Dtr operon, and *tra* box II and *tra* box III of the Mpf operon. So far, $TraR_{NGR}$ has been shown to activate a promoter containing the *tra* box II sequence [23]. The *tra* box II element is an 18-bp imperfect inverted repeat, located upstream of the *traI* gene which encodes a LuxI-type AHL synthase, the first structural gene of the Mpf operon on pNGR234a.

Electrophoretic mobility shift assays (EMSA) showed that $TraR_{NGR}$ formed a complex with a 558-bp *traI* promoter DNA, which includes the sequence of *tra* box II, but did not associate with a 214-bp DNA of unrelated sequence (Fig. 1A). These findings indicate that binding of $TraR_{NGR}$ to the *traI* promoter is specific. To further characterize the thermodynamics of TraR–DNA interaction, we constructed a 20-bp DNA duplex that contains one extra base pair flanking both ends of *tra* box II. Isothermal calorimetry (ITC) revealed that $TraR_{NGR}$ interacted with this DNA with a dissociation constant (K_d) of 175.1 ± 32.5 nM (Fig. 1B). This affinity is similar to that of $TraR_{At}$–DNA from *A. tumefaciens*. The ITC-derived K_d of $TraR_{At}$ with an 18 bp-DNA duplex containing the cognate tra_{At} box is 220.3 ± 23.5 nM (data not shown); this same 18-bp duplex sequence was used to form the $TraR_{At}$–DNA complex for crystallographic studies [14,15]. Moreover, our ITC study showed that two $TraR_{NGR}$ monomers, or one $TraR_{NGR}$ dimer, were associated with one DNA (Fig. 1B and also Table 1), consistent with the crystal structure of $TraR_{At}$–DNA where one $TraR_{At}$ dimer interacts with the two half-sites of the inverted repeat in the two neighboring major grooves of DNA [14,15].

3.2. TraR K213 is involved in DNA binding

In the structure of $TraR_{At}$–DNA [14,15], two Arg residues (R206 and R210) make specific contact with bases in DNA *via* H-bond,

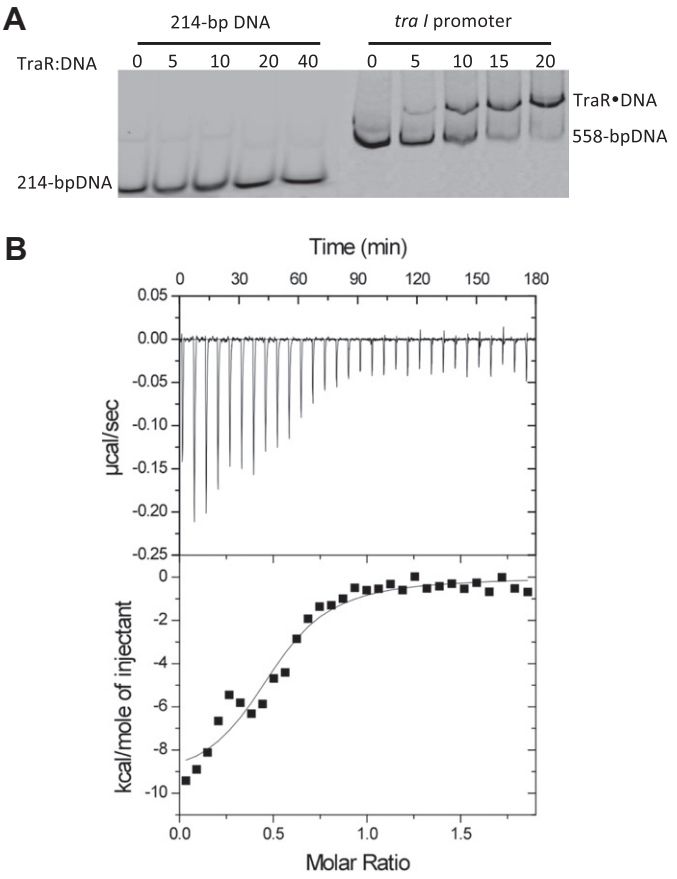

Fig. 1. Specific binding of $TraR^{wt}_{NGR}$ with DNA. (A) Titration of the 558-bp *tral* promoter DNA and a 214-bp DNA with various amounts of $TraR^{wt}_{NGR}$ by EMSA. The 214-bp DNA is the *blcABC* promoter used in an unrelated study. The concentration of both DNA fragments was kept at 100 nM. Lane 1 and 6, DNA only; Lanes 2–5 and 7–10, $TraR_{NGR}$:DNA molar ratios as indicated above the lanes. (B) ITC studies of $TraR^{wt}_{NGR}$ with the 20-bp DNA containing the *tra* box II sequence.

Table 1
ITC-derived thermodynamic parameters of TraR–DNA interaction and TraR–TraM interaction using various TraR proteins.

TraR proteins	With the 20 bp DNA[a]		With $TraM^{wt}$ [b]	
	TraR:DNA[c]	K_d (nM)	TraM:TraR[c]	K_d (nM)
$TraR^{wt}_{NGR}$	2.2 ± 0.1	175.1 ± 32.5	1.0 ± 0.1	12.2 ± 2.9
$TraR^{P178A}_{NGR}$	2.0 ± 0.1	115.9 ± 13.9	1.0 ± 0.1	133.2 ± 26.9
$TraR^{L182A}_{NGR}$	2.0 ± 0.1	196.1 ± 49.0	1.2 ± 0.1	400.0 ± 61.0
$TraR^{W186A}_{NGR}$	2.0 ± 0.1	190.5 ± 42.4	1.0 ± 0.1	662.2 ± 215.8
$TraR^{L199A}_{NGR}$	1.8 ± 0.1	135.1 ± 30.9	1.0 ± 0.1	261.1 ± 30.2

[a] The 20 bp DNA containing *tra* box II was titrated into $TraR_{NGR}$ proteins.
[b] The $TraR_{NGR.}$ proteins were titrated into $TraR^{wt}_{NGR}$.
[c] Concentrations of $TraR_{NGR}$ and Tra_{MNGR} were expressed in the monomeric form.

suggesting a mechanism for $TraR_{At}$ to recognize the tra_{At} sequence on DNA. Based on the sequence alignment, the R206 and R210 equivalents in $TraR_{NGR}$ are Q208 and D212 (Fig. 2A); although both are capable of participating in H-bonding interactions with bases, the negative charged Asp is not favorable in general for interacting with negatively charged DNA. Immediately adjacent to D212 is K213 and lysines commonly function in DNA binding. To identify the DNA-binding residues in $TraR_{NGR}$, we substituted Q208, D212 and K213 with Ala, and examined the DNA-binding property of these variants.

Both $TraR^{Q208A}_{NGR}$ and $TraR^{D212A}_{NGR}$ maintained the wild-type affinity in binding the 20-bp DNA by ITC (K_ds of 126.7 ± 14.2 and 125.9 ± 25.3 nM, respectively), and bound the *tral* promoter DNA in the similar manner as $TraR^{wt}_{NGR}$ based on EMSA studies (Supplementary Fig. S1). In contrast, mutation of K213A diminished TraR–DNA interactions as indicated by the lack of heat exchange in the ITC experiments (Fig. 2B). Consistently, EMSA studies show $TraR^{K213A}_{NGR}$ did not effectively interact with the *tra* box II DNA sequence (Fig. 2C). These findings suggest that $TraR_{NGR}$ K213, but not Q208 or D212, is important for binding of $TraR_{NGR}$ to DNA.

We next examined whether the DNA-binding important residue K213 was involved in interaction with $TraM_{NGR}$. The K213A mutation did not affect $TraR_{NGR}$–$TraM_{NGR}$ interaction, as $TraR^{K213A}_{NGR}$ bound TraM with a similar affinity (K_d of 19.3 ± 2.9 nM) as $TraR^{wt}_{NGR}$ (12.2 ± 2.9 nM). The findings that $TraR_{NGR}$ K213 is indispensible for DNA interaction but not for forming complex with $TraM_{NGR}$ are in agreement with structural analysis that the DNA and the TraM binding sites on TraR do not overlap [22].

3.3. $TraR_{NGR}$ residues that are critical in interacting with $TraM_{NGR}$

Although $TraM_{NGR}$ interacts with both NTD and CTD of $TraR_{NGR}$ in the crystal structure of the $TraR_{NGR}$–$TraM_{NGR}$ complex, the $TraM_{NGR}$–CTD interaction is more stable and specific [22]. We therefore focused on the $TraM_{NGR}$–CTD interface: side chains of $TraR_{NGR}$ P178, L182, W186, and L199 interact with residues from $TraM_{NGR}$. To confirm the structural observations, these residues were mutated to Ala and the mutational effects on $TraR_{NGR}$–$TraM_{NGR}$ interaction were examined. Individual mutations of these four residues decreased the binding affinity of $TraR_{NGR}$ for $TraM_{NGR}$ by ~10–50-fold (Table 1; Fig. 3A for an example). The weakened interactions between these $TraR_{NGR}$ mutants and $TraM_{NGR}$ accounted for the increased amounts of $TraM_{NGR}$ required to dissociate $TraR_{NGR}$–DNA in EMSA studies (Fig. 3B, C). Importantly, these $TraR_{NGR}$ mutants maintained the wild type binding of DNA based on EMSA studies (Supplementary Fig. S2), supporting the proposal that TraR has separate binding surfaces for DNA and TraM.

3.4. The W186 and L199 interfaces

The $TraR_{NGR}$–$TraM_{NGR}$ structure indicates that $TraR_{NGR}$ W186 and L199 each interact with multiple $TraM_{NGR}$ residues [22]. To further investigate the role of the $TraR_{NGR}$ W186 and L199 interfaces in TraR–TraM complex formation, we next mutated their respective contacting $TraM_{NGR}$ residues. $TraR_{NGR}$ W186 specifically interacts with $TraM_{NGR}$ H39 and Q85 *via* hydrogen bonding, in addition to numerous van der Waals contacts [22]. When H39 or Q85 were mutated with hydrophobic residues of Ala or Leu, the resulting proteins ($TraM^{H39A}_{NGR}$, $TraM^{H39L}_{NGR}$ and $TraM^{Q85A}_{NGR}$) maintained the binding affinity for $TraR_{NGR}$ similar to that of $TraM^{wt}_{NGR}$ (Table 2). Mutation of either residue to the charged amino acid of Glu decreased the $TraR_{NGR}$–$TraM_{NGR}$ interaction by ~4.5-fold. When the polar nature was preserved in substitution, $TraM^{H39Q}_{NGR}$ maintained the wild-type binding affinity for $TraR_{NGR}$; however, $TraM^{Q85N}_{NGR}$ displayed a 5-fold reduction in binding to $TraR_{NGR}$ (Table 2). Thus, substitutions of H39 and Q85 with amino acids of various properties affected the $TraR_{NGR}$–$TraM_{NGR}$ interaction moderately with a maximum scale of 5-fold reduction. Consistent with the modest role of H39 and Q85 in binding of $TraR_{NGR}$, EMSA studies showed that all the $TraM_{NGR}$ H39 and Q85 variants were able to displace $TraR_{NGR}$ from the pre-formed TraR–DNA complex (see Supplementary Fig. S3A for example).

$TraR_{NGR}$ L199 extends its side chain into a hydrophobic pocket formed by residues including L88, L92, L95, V98 and P99 of the TraM C-terminus [22]; the hydrophobic C-terminal tail of $TraM_{At}$ has been shown to be functionally important [20]. Mutations of these $TraM_{NGR}$ residues to Ala decreased the binding affinity of $TraM_{NGR}$ for $TraR_{NGR}$ to various extents with the largest 10-fold

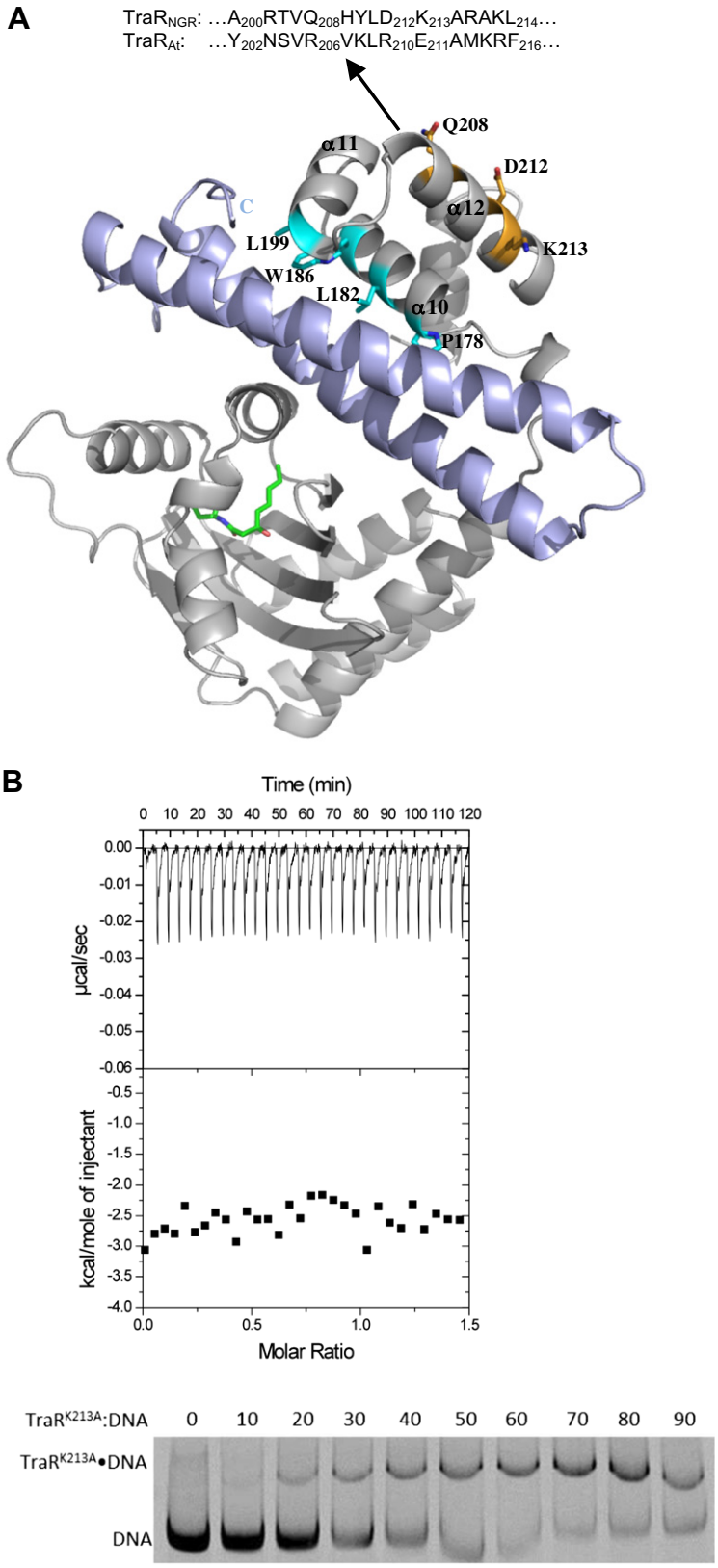

Fig. 2. Mutation of K213A diminished TraR$_{NGR}$–DNA interaction. (A) Position of K213 in the structure of TraR$_{NGR}$–TraM$_{NGR}$ complex (PDB code 2Q0O). Shown here is the association of TraR$_{NGR}$ with TraM$_{NGR}$ in the closed conformation, where TraM$_{NGR}$ interacts with both the N- and C-terminal domains of the TraR$_{NGR}$ monomer [22]. Shown are side chains of Q208, D212, K213 (orange), P178, L182, W186, and L199 (cyan) (the four being the TraM-interacting residues). 3-oxo-C8-HSL is colored green, the TraR$_{NGR}$ monomer is gray, and TraM$_{NGR}$ is light blue. Insert: sequence alignment of TraR$_{NGR}$ and TraR$_{At}$ in the DNA binding helix (α12). (B) ITC studies of TraR$^{K213A}_{NGR}$ binding with the 20-bp DNA. (C) Titration of the 551-bp *traI* promoter DNA with various amounts of TraR$^{K213A}_{NGR}$ by EMSA. The concentration of DNA was kept at 100 nM.

reduction found in the L92A substitution (Table 2). The weakened affinities, however, did not prevent these TraM$_{NGR}$ variants from displacing TraR$_{NGR}$ from DNA based on EMSA studies (Supplementary Fig. S3B).

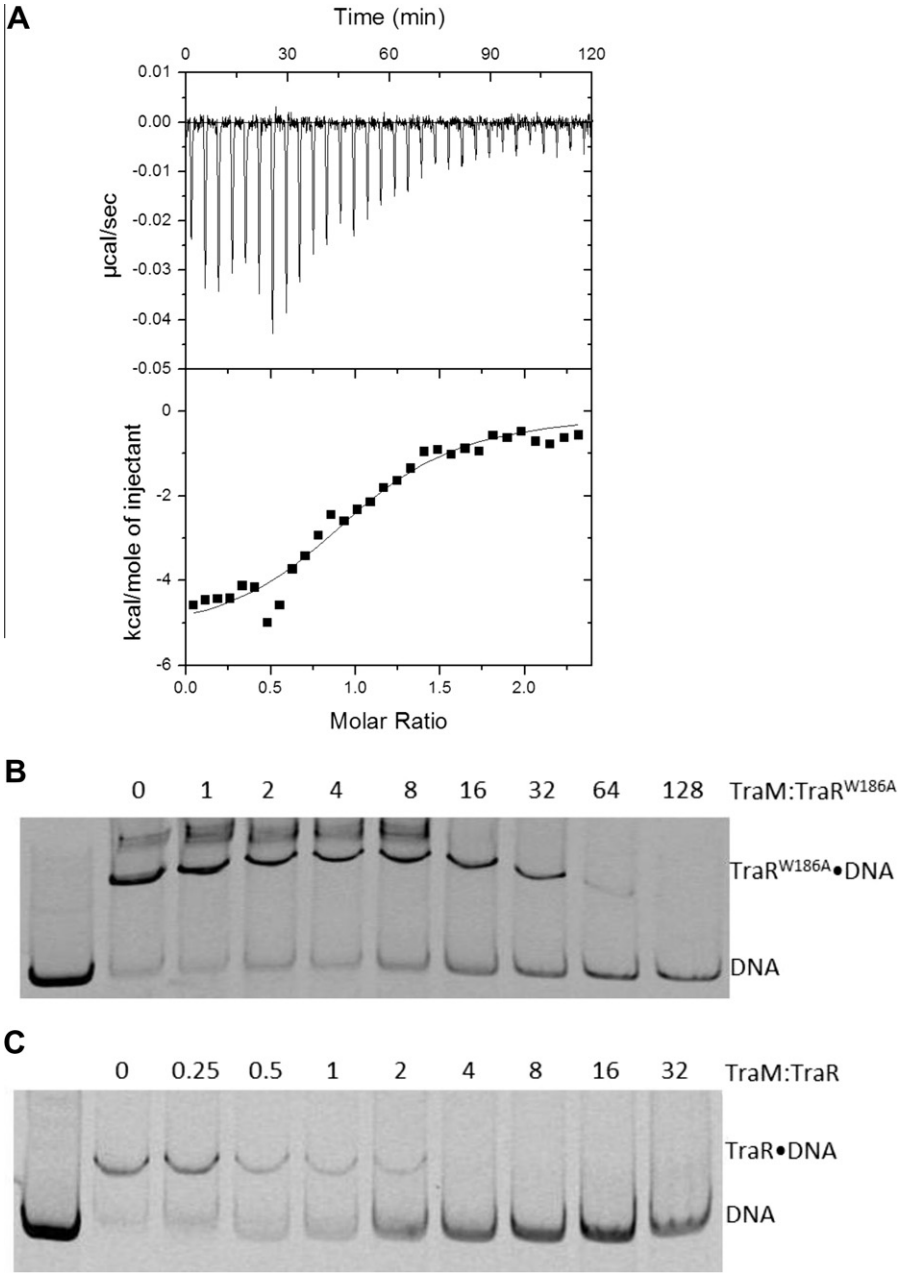

Fig. 3. Mutations of W186A drastically decreased $TraR_{NGR}$–$TraM_{NGR}$ interaction. (A) ITC studies of $TraR^{W186A}_{NGR}$–$TraM_{NGR}$ interaction; (B, C) EMSA studies of TraM titration into the $TraR^{W186A}_{NGR}$–DNA and $TraR^{wt}_{NGR}$–DNA complexes. Lane 1, DNA only; Lane 2, DNA–$TraR_{NGR}$ complex in the molar ratio of DNA:TraR = 1:30; Lanes 3–10, DNA–$TraR_{NGR}$ in the presence of various amounts of $TraM_{NGR}$. The concentration of DNA was kept at 100 nM. The ratios indicated above the lanes refer to the molar ratios of $TraR_{NGR}$:$TraM_{NGR}$.

In summary, of the structurally observed $TraR_{NGR}$-interacting residues, we found the contribution from individual $TraM_{NGR}$ residues to the $TraR_{NGR}$–$TraM_{NGR}$ interaction or to inhibiting DNA-binding activity of $TraR_{NGR}$ was modest. Interestingly, mutations of $TraM_{At}$ H40 and P97, the $TraM_{NGR}$ H39 and P99 equivalents, have been shown to abolish the inhibitory function of $TraM_{At}$ on the DNA-binding activity of $TraR_{At}$, although $TraM_{At}^{H40A}$ maintains stable interaction with $TraR_{At}$ [20].

4. Discussion

The activity of the quorum sensing transcription factor TraR of the *Rhizobiaceae* family can be inhibited by anti-activator TraM through protein-protein interaction. Prior structural analysis on the activation ($TraR_{At}$–DNA) and the anti-activation ($TraR_{NGR}$–$TraM_{NGR}$) complexes of two homologous systems suggests that TraR uses separate surfaces for the binding of DNA and TraM, and an allosteric mechanism for TraM to inhibit TraR from binding to DNA has been proposed [22]. Here, we identified a DNA-binding $TraR_{NGR}$ residue, and found that it is separated from the $TraM_{NGR}$-binding site. We further confirmed that the interfaces are independent by showing that the DNA-binding impaired $TraR_{NGR}$ variant binds $TraM_{NGR}$ as strongly as $TraR^{wt}_{NGR}$, and that the $TraM_{NGR}$-binding deficient $TraR_{NGR}$ variants retain wild-type DNA binding affinity. While analyzing the $TraR_{NGR}$–$TraM_{NGR}$ interface, we found that mutations of individual $TraR_{NGR}$ or $TraM_{NGR}$ residues do not abolish the $TraR_{NGR}$–$TraM_{NGR}$ interaction. Mutations of $TraR_{NGR}$ residues decrease the $TraR_{NGR}$–$TraM_{NGR}$ interaction greater than those of $TraM_{NGR}$ residues, consistent with the structural observations that each $TraR_{NGR}$ residue interacts with more $TraM_{NGR}$ residues than each $TraM_{NGR}$ with $TraR_{NGR}$.

Results from our mutational analyses of $TraR_{NGR}$ and $TraM_{NGR}$ have several differences when compared with those reported for

Table 2
Mutational analysis of TraMNGR mutants in binding to TraRNGR by ITC.

TraM proteins	Kd (nM)	Stoichiometry
$TraR_{NGR}^{wt}$	12.2 + 2.9	1.0 + 0.1
$TraR_{NGR}^{H39A}$	13.9 + 2.5	1.0 + 0.1
$TraR_{NGR}^{H39L}$	24.1 + 6.0	0.9 + 0.1
$TraR_{NGR}^{H39E}$	52.1 + 13.0	1.0 + 0.1
$TraR_{NGR}^{H39Q}$	16.9 + 3.4 1	1.0 + 0.1
$TraR_{NGR}^{Q85A}$	23.3 + 4.3	1.1 + 0.1
$TraR_{NGR}^{Q85E}$	57.8 + 13.2	1.0 + 0.1
$TraR_{NGR}^{Q85N}$	59.2 + 6.0	0.9 + 0.1
$TraR_{NGR}^{L88A}$	70.9 + 8.2	0.8 + 0.1
$TraR_{NGR}^{L92A}$	112.9 + 17.3	0.9 + 0.1
$TraR_{NGR}^{L95A}$	37.7 + 3.5	0.8 + 0.1
$TraR_{NGR}^{V98A}$	31.0 + 4.6	1.0 + 0.1
$TraR_{NGR}^{P99A}$	42.4 + 6.0	1.0 + 0.1

$TraR_{NGR}^{wt}$ was titrated into $TraM_{NGR}$ variants. Concentrations of $TraR_{NGR}$ and $TraM_{NGR}$ proteins were expressed in the monomeric form.

the *A. tumefaciens* homologues. Individual residues in $TraM_{At}$ have been shown to strongly affect the inhibitory activity of $TraM_{At}$ on $TraR_{At}$ [20,21,24,25]. In particular, in vivo studies show that mutations of H40A or P97A or P97S, corresponding to H39 and P99 of $TraM_{NGR}$, abrogate the inhibition of $TraM_{At}$ on $TraR_{At}$. Interestingly, $TraM_{At}^{H40A}$ retains strong affinity for $TraR_{At}$ with an apparent K_d of 47 nM (K_d of ~4 nM for $TraM_{At}^{wt}$ with $TraR_{At}$; both derived from surface plasmon resonance). In addition, $TraM_{At}^{Q82A}$ (Q82 is related to Q85 of $TraM_{NGR}$) fails to inhibit TraR transcription activity despite its strong interaction with $TraR_{At}$ [20,25]. The impairment of $TraM_{At}^{Q82A}$ has been attributed to its inefficiency in converting the $TraR_{At}$–DNA complex to the anti-activation $TraR_{At}$–$TraM_{At}$ complex, due to the formation of a stable ternary DNA–$TraR_{At}$–$TraM_{At}$ intermediate [25]. Divergent mutational results are also observed for TraR proteins of the NGR234 and *A. tumefaciens* systems. For example, a W186A mutation in $TraR_{NGR}$ weakens the $TraR_{NGR}$–$TraM_{NGR}$ interaction by ~55-fold based on our ITC studies here, however, the corresponding W184A mutation of $TraR_{At}$ does not influence $TraR_{At}$ binding to $TraM_{At}$ based on far western analysis [25]. It is possible that the mutational effect of $TraR_{At}$ W184A was not revealed by the limited resolution provided through the far western technique. In addition, structural dissimilarities are also found between the two systems. $TraM_{NGR}$ is found as stable monomer in solution whereas $TraM_{At}$ is homodimeric [22,26,27], and the $TraR_{NGR}$–$TraM_{NGR}$ complex is tetrameric while the $TraR_{At}$–$TraM_{At}$ complex is octomeric. Finally $traR_{NGR}$ may be inhibited by co-expression of $traM_{NGR}$, but not by co-expression of $traM_{At}$ [23]. Despite these mutational, structural and functional differences, TraM anti-activation in both systems is driven thermodynamically. The TraR–TraM complexes are thermodynamically more stable (K_d of 12.2 and 3.7 nM [27] for the NGR234 and *A. tumefaciens* complexes, respectively) than TraR-DNA (K_d of 175.1 and 220.3 nM for the NGR234 and *A. tumefaciens* complexes, respectively).

Acknowledgment

This work was supported by a Grant (MCB-0416447) from NSF to L.C.

Appendix A. Supplementary data

Supplementary data associated with this article can be found, in the online version, at doi:10.1016/j.bbrc.2012.01.035.

References

[1] G.M. Dunny, S.C. Winans (Eds.), Cell–Cell Signaling in Bacteria, Amercian Society for Microbiology, Washington, DC, 1999.
[2] M.B. Miller, B.L. Bassler, Quorum sensing in bacteria, Annu. Rev. Microbiol. 55 (2001) 165–199.
[3] C. Fuqua, E.P. Greenberg, Listening in on bacteria: acyl-homoserine lactone signalling, Nat. Rev. Mol. Cell Biol. 3 (2002) 685–695.
[4] J. Engebrecht, M. Silverman, Identification of genes and gene products necessary for bacterial bioluminescence, Proc. Natl. Acad. Sci. USA 81 (1984) 4154–4158.
[5] A.L. Schaefer, D.L. Val, B.L. Hanzelka, J.E. Cronan Jr., E.P. Greenberg, Generation of cell-to-cell signals in quorum sensing: acyl homoserine lactone synthase activity of a purified Vibrio fischeri LuxI protein, Proc. Natl. Acad. Sci. USA 93 (1996) 9505–9509.
[6] C. Fuqua, E.P. Greenberg, Signal generation in autoinduction systems: synthesis of acylated homoserine lactones by LuxI-type proteins, in: G.M. Dunny, S.C. Winans (Eds.), Cell–Cell Signaling in Bacteria, ASM Press, Washington, DC, 1999, pp. 211–230.
[7] H.B. Kaplan, E.P. Greenberg, Diffusion of autoinducer is involved in regulation of the Vibrio fischeri luminescence system, J. Bacteriol. 163 (1985) 1210–1214.
[8] J.P. Pearson, C. Van Delden, B.H. Iglewski, Active efflux and diffusion are involved in transport of Pseudomonas aeruginosa cell-to-cell signals, J. Bacteriol. 181 (1999) 1203–1210.
[9] M.E. Churchill, L. Chen, Structural basis of acyl-homoserine lactone-dependent signaling, Chem. Rev. 111 (2011) 68–85.
[10] J.H. Devine, G.S. Shadel, T.O. Baldwin, Identification of the operator of the lux regulon from the Vibrio fischeri strain ATCC7744, Proc. Natl. Acad. Sci. USA 86 (1989) 5688–5692.
[11] K.R. Piper, S. Beck von Bodman, S.K. Farrand, Conjugation factor of Agrobacterium tumefaciens regulates Ti plasmid transfer by autoinduction, Nature 362 (1993) 448–450.
[12] W.C. Fuqua, S.C. Winans, A LuxR-LuxI type regulatory system activates Agrobacterium Ti plasmid conjugal transfer in the presence of a plant tumor metabolite, J. Bacteriol. 176 (1994) 2796–2806.
[13] A.M. Stevens, E.P. Greenberg, Transcriptional activation by TraR, in: G.M. Dunny, S.C. Winans (Eds.), Cell–Cell Signaling in Bacteria, ASM Press, Washington DC, 1999, pp. 231–242.
[14] R.G. Zhang, T. Pappas, J.L. Brace, P.C. Miller, T. Oulmassov, J.M. Molyneaux, J.C. Anderson, J.K. Bashkin, S.C. Winans, A. Joachimiak, Structure of a bacterial quorum-sensing transcription factor complexed with pheromone and DNA, Nature 417 (2002) 971–974.
[15] A. Vannini, C. Volpari, C. Gargioli, E. Muraglia, R. Cortese, R. De Francesco, P. Neddermann, S.D. Marco, The crystal structure of the quorum sensing protein TraR bound to its autoinducer and target DNA, Embo J 21 (2002) 4393–4401.
[16] J. Zhu, S.C. Winans, Autoinducer binding by the quorum-sensing regulator TraR increases affinity for target promoters in vitro and decreases TraR turnover rates in whole cells, Proc. Natl. Acad. Sci. USA 96 (1999) 4832–4837.
[17] I. Hwang, D.M. Cook, S.K. Farrand, A new regulatory element modulates homoserine lactone-mediated autoinduction of Ti plasmid conjugal transfer, J. Bacteriol. 177 (1995) 449–458.
[18] C. Fuqua, M. Burbea, S.C. Winans, Activity of the Agrobacterium Ti plasmid conjugal transfer regulator TraR is inhibited by the product of the traM gene, J. Bacteriol. 177 (1995) 1367–1373.
[19] Z.Q. Luo, Y. Qin, S.K. Farrand, The antiactivator TraM interferes with the autoinducer-dependent binding of TraR to DNA by interacting with the C-terminal region of the quorum-sensing activator, J. Biol. Chem. 275 (2000) 7713–7722.
[20] A. Swiderska, A.K. Berndtson, M.R. Cha, L. Li, G.M. Beaudoin 3rd, J. Zhu, C. Fuqua, Inhibition of the Agrobacterium tumefaciens TraR quorum-sensing regulator. Interactions with the TraM anti-activator, J. Biol. Chem. 276 (2001) 49449–49458.
[21] I. Hwang, A.J. Smyth, Z.Q. Luo, S.K. Farrand, Modulating quorum sensing by antiactivation: TraM interacts with TraR to inhibit activation of Ti plasmid conjugal transfer genes, Mol. Microbiol. 34 (1999) 282–294.
[22] G. Chen, P.D. Jeffrey, C. Fuqua, Y. Shi, L. Chen, Structural basis for antiactivation in bacterial quorum sensing, Proc. Natl. Acad. Sci. USA 104 (2007) 16474–16479.
[23] X. He, W. Chang, D.L. Pierce, L.O. Seib, J. Wagner, C. Fuqua, Quorum sensing in Rhizobium sp. strain NGR234 regulates conjugal transfer (tra) gene expression and influences growth rate, J. Bacteriol. 185 (2003) 809–822.
[24] Y. Qin, A.J. Smyth, S. Su, S.K. Farrand, Dimerization properties of TraM the antiactivator that modulates TraR,-mediated quorum-dependent expression of the Ti plasmid tra genes, Mol. Microbiol. 53 (2004) 1471–1485.
[25] Y. Qin, S. Su, S.K. Farrand, Molecular basis of transcriptional antiactivation TraM disrupts the TraR–DNA complex through stepwise interactions, J. Biol. Chem. 282 (2007) 19979–19991.
[26] G. Chen, J.W. Malenkos, M.R. Cha, C. Fuqua, L. Chen, Quorum-sensing antiactivator TraM forms a dimer that dissociates to inhibit TraR, Mol. Microbiol. 52 (2004) 1641–1651.
[27] G. Chen, C. Wang, C. Fuqua, L.H. Zhang, L. Chen, Crystal structure and mechanism of TraM2, a second quorum-sensing antiactivator of Agrobacterium tumefaciens strain A6, J. Bacteriol. 188 (2006) 8244–8251.